(41) Holyer, R. H.; Hubbard, C. D.; Kettle, S. F.; Wilkins, R. G. *Inorg. Chem.* **1966**, *5*, 622.
(42) Hubbard, C. D.; Pacheco, D. *J. Inorg. Nucl. Chem.* **1977**, *39*, 1373.
(43) Cobb, M. A.; Hague, D. N. *Trans. Faraday Soc.* **1971**, *67*, 3069.
(44) Cobb, M. A.; Hague, D. N. *J. Chem. Soc. Faraday Trans. 1* **1972**, *68*, 932.
(45) James, A. D.; Robinson, B. H. *J. Chem. Soc., Faraday Trans. 1* **1978**, *74*, 10.
(46) Eigen, M. *Pure Appl. Chem.* **1963**, *6*, 97. Eigen, M.; Wilkins, R. G. *Adv. Chem. Ser.* **1965**, *No. 49*, 55.
(47) p*K* values for the protonation of the ring nitrogen and for ionization of the hydroxyl group are respectively 2.32 and 12.0 in 50/50 water–methanol (ref 48) and 2.0 and 12.3 in 50/50 water–dioxane (ref 42).
(48) Anderson, R. G.; Nickless, G. *Analyst (London)* **1968**, *93*, 13.
(49) Hnilickova, M.; Sommer, L. *Collect. Czech. Chem. Commun.* **1961**, *26*, 2189.
(50) Yamagishi, A. *J. Phys. Chem.* **1981**, *85*, 2665.
(51) See for instance: Ise, N. In "Charged and Reactive Polymers"; Rembaum, A., Selegny, E., Eds.; D. Reidel: Dordrecht, Holland, 1975; Vol. 2 and references therein.
(52) Tondre, C.; Sbiti, N. *Polym. Prepr., Am. Chem. Soc., Div. Polym. Chem.* **1982**, *23*, 67.
(53) Manning, G. S. In "Charged and Reactive Polymers"; Selegny, E., Ed.; D. Reidel: Dordrecht, Holland, 1974; Vol. 1, p 14.
(54) Manning, G. S. *J. Chem. Phys.* **1969**, *51*, 924.
(55) Baumgartner, E.; Fernandez-Prini, R.; Turyn, D. *J. Chem. Soc., Faraday Trans. 1* **1974**, *70*, 1518.
(56) Conio, G.; Patrone, E.; Russo, S.; Trefiletti, V. *Makromol. Chem.* **1976**, *177*, 49.
(57) Tondre, C.; Zana, R. *J. Phys. Chem.* **1971**, *75*, 3367.
(58) Diekmann, S.; Frahm, J. *J. Chem.* Soc., *Faraday Trans. 1* **1979**, *75*, 2199.
(59) Kunugi, S.; Ise, N. *Z. Phys. Chem. (Frankfurt/Main)* **1974**, *92*, 69.

Ellipsometry Studies of Adsorbed Polymer Chains Subjected to Flow

Jen-Jiang Lee and Gerald G. Fuller*

Department of Chemical Engineering, Stanford University, Stanford, California 94305.
Received February 23, 1983

ABSTRACT: Ellipsometry has been applied to study the average thickness of adsorbed polymer layers under flowing conditions. The measurement also produces a simultaneous determination of the surface concentration. Measurements have been conducted under flowing pure solvent at the Θ-temperature on four polystyrene samples of molecular weights ranging from 1.8×10^6 to 20×10^6 adsorbed previously onto chrome from quiescent cyclohexane solutions. No detectable changes in film thickness were observed for the three lower molecular weight samples over the whole range of velocity gradients applied. On the other hand, the film thickness of the 20 million molecular weight sample began to decrease as the apparent velocity gradient surpassed 2000 s^{-1} and decreased as much as 15% when the apparent velocity gradient reached 7800 s^{-1}. The response of the adsorbed polymer layer to the imposition of the flow over short periods of time was reversible, and no change in adsorbance was observed between the inception and cessation of the flow. The measured conformational changes were also compared to the predictions of a simple bead-and-spring model of an attached polymer segment, and qualitative agreement was obtained when the effect of finite extensibility was included in the model.

Introduction

Polymer adsorption has been the focus of considerable attention in recent years because of a large number of processes in which this phenomenon is important. The majority of work, however, has been devoted to the case of adsorbed chains in quiescent systems, and relatively few studies have considered the effect of hydrodynamic forces on the adsorbed layer. Since most applications in which polymer adsorption is important involve the presence of a flow field (enhanced oil recovery, lubrication, liquid chromatography, and filtration), there is a need for understanding the interactions of the dangling ends and loose loops making up the adsorbed layer of polymer chains and hydrodynamic forces arising from the flow of liquid above the solid–liquid interface.

Hydrodynamic forces can affect the adsorbed layer in one of two ways. The first case is one in which the polymer chains are first adsorbed under no-flow conditions and then subjected to the flow of the bulk liquid above the surface. For a weakly adsorbed, high molecular weight, flexible chain (the case often encountered in industrial applications), only a small proportion of the polymer segments is actually attached to the surface with the remainder extending away from the surface as dangling ends or loose loops. The imposition of hydrodynamic forces can result in distortion and alignment of those unattached segments. Furthermore, if the shear stress is large enough, it is conceivable that the chains could be torn away from the surface.

The second case where the importance of flow should be investigated is one where the chains are adsorbed from a flowing solution. This could result in flow-induced deformation and orientation of the polymer chains prior to attachment to the surface. It is possible that such changes in conformation could affect both the kinetics of the adsorption and the final conformation of the film. This paper is strictly concerned with the first case, where the polymer is adsorbed from quiescent solutions. The second case will be the subject of a later paper.

The previous studies in this area which most convincingly demonstrate the possibility of flow-induced changes in the conformation of polymer films are those reported by Gramain and Myard[1] and, more recently, by Cohen and Metzner.[2] In both studies, a simple hydrodynamic method was used to infer the properties of polymer films in the presence of flow. This is carried out by measuring the pressure drop required to sustain a given flow rate through either a porous media[1] or a capillary tube.[2] From such measurements, the effective hydrodynamic thickness of an adsorbed layer can be estimated if it is assumed that the increased hydrodynamic resistance due to the film comes about solely from a constriction of the path through which the fluid is flowing by the adsorbed polymer layer. The study of Gramain and Myard[1] utilized the flow of pure

0024-9297/84/2217-0375$01.50/0

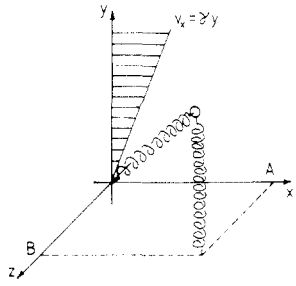

Figure 1. Schematic of the dumbbell model—a dangling end is simulated by setting $A = B = 0$.

solvent through various membranes containing adsorbed polymer. At low flow rates a linear relationship between pressure drop and flow rate was observed, indicating a constant hydrodynamic thickness. At very large velocity gradients a greater than linear pressure drop response with flow rate was reported. This positive deviation indicated flow-induced deformation of the adsorbed layer in such a manner as to increase the hydrodynamic resistance of the film. Gramain and Myard[1] further suggested that the mechanism by which this occurred was an increase in the hydrodynamic thickness of the film.

The experiments of Cohen and Metzner,[2] on the other hand, consisted of flowing moderately concentrated polymer solutions through fine capillaries. With use of an analysis by which shear thinning and wall slip was included in the calculations, an effective hydrodynamic thickness of an adsorbed layer was evaluated. This effective thickness was reported, however, to decrease with increased velocity gradients in contrast to the dilatant behavior observed by Gramain and Myard. Although the two experiments cannot be directly compared due to different experimental conditions employed by the two groups, these results do suggest more research is needed in order to better understand the conformation of adsorbed chains in flowing environments.

The intent of the work presented in this paper was to employ a nonperturbing optical method, ellipsometry, to the study of polymer films subjected to flow. Unlike the hydrodynamic method, where film thickness can only be inferred through measurement of hydrodynamic resistance, ellipsometry offers the possibility of directly measuring the average film thickness. In addition, the refractive index of the film can be determined which, together with the film thickness measurement, can be used to estimate the adsorbance or surface concentration of the film. These simultaneous measurements may provide less ambiguous evidence on how the adsorbed layer responds to a flow field in terms of the average film thickness and surface concentration. We have also complemented the experiments with a simple bead-and-spring model of an adsorbed polymer chain which is able to qualitatively describe the observed flow-induced conformational changes.

Finitely Extensible Bead-and-Spring Model of an Adsorbed Chain. The simplest model that can be devised to represent the dynamics of either a dangling end or loop attached to a surface is the bead-and-spring model first proposed for this purpose by DiMarzio and Rubin.[3] This model, pictured in Figure 1, has all the frictional resistance of the chain embedded at a single point in space. This bead is then attached to the surface by a spring with force coefficient $K(r)$, which in general is a function of the end-to-end distance of the spring for reasons that will be brought out later. When a single spring is used, a dangling end is modelled whereas a loop attached to the surface can be described by using two separate springs to tether the bead to the surface. Since the qualitative results for a loop and a dangling end are the same, only the dangling end will be described here. The conformation of the attached chain is described through a probability distribution function $\Psi(\mathbf{r},t)$, which prescribes the likelihood that the bead is at a position $\mathbf{r}$ at time t. The diffusion equation describing the evolution of Ψ is

$$\frac{\partial \Psi}{\partial t} + \dot{\gamma} y' \frac{\partial \Psi}{\partial x'} - \frac{1}{\beta} \nabla \cdot K(r') \mathbf{r}' \Psi - \frac{kT}{\beta} \nabla^2 \Psi = 0 \qquad (1)$$

where $\dot{\gamma}$ is the velocity gradient in the y-direction of a simple shear flow in the x-direction, β is the friction coefficient, and kT is the Boltzmann temperature factor. The influence of the bounding surface is incorporated into the problem by imposing the following no flux boundary condition:

$$(\partial \Psi / \partial y')_{y'=0} = 0 \qquad (2)$$

This model is among the simplest possible and is deficient for a number of reasons. A major problem with the model is that only a single, isolated chain can be described whereas in reality the adsorbed layers typically consist of chains that are in very close proximity to each other and which most likely overlap. The major advantage of this model is that it can be handled analytically, and in spite of its shortcomings, the model predictions may offer qualitative indications of the mechanisms by which adsorbed chains respond to flow.

Although the solution of eq 1 subject to eq 2 is very difficult, Fuller[4] has recently demonstrated that exact solutions for the moments of Ψ can be obtained for the case of a linear spring where $K(r)$ is replaced by a constant K_0. The solutions for moments of interest are

$$\langle x^2 \rangle = (1/2N)[1 + (\alpha^2/8)] \qquad (3)$$

$$\langle y^2 \rangle = \langle z^2 \rangle = 1/2N \qquad (4)$$

$$\langle xy \rangle = (1/8N)\alpha \qquad (5)$$

where $\alpha = 2\beta\dot{\gamma}/K_0$ is the dimensionless velocity gradient. The length scales in eq 3–5 have been normalized by L, which is the contour length of the chain. The parameter N is defined as $L^2/(2kT/K_0)$ and can be shown to be proportional to the molecular weight of the chain for the case of a Gaussian coil.

Since the thickness of the adsorbed layer is proportional to $\langle y^2 \rangle^{1/2}$, the model predicts the thickness will remain unchanged by the flow even though the segments do distort and align as indicated by the α dependence of the moments $\langle xy \rangle$ and $\langle x^2 \rangle$. The reason for this prediction is that the constant spring coefficient K_0 allows the segment to deform without bound. This is physically unrealistic since the end-to-end distance of the spring must be ultimately bounded by the contour length of the chain. This constraint has been recognized in the past with models of dilute polymer solutions, and a conformation dependent spring coefficient is introduced in order to incorporate finite extensibility. The principal requirements of such a coefficient are that it should be relatively constant for small values of r but should approach an infinite value as $|\mathbf{r}| \rightarrow 1$ where r has been normalized by L. A commonly used functional form for K is the following one proposed by Warner:[5]

$$K(r) = K_0/(1 - r^2) \qquad (6)$$

When the above form for $K(r)$ is introduced into eq 1 it is no longer possible to obtain analytical results for the moments of Ψ. The method that has been adopted in the past in order to obtain approximate solutions is to replace

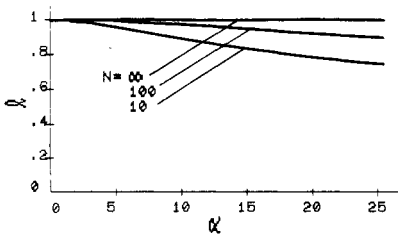

Figure 2. Model prediction of film thickness ratio l as a function of dimensionless velocity gradient α using a Warner spring for $N = 10$, 100, and ∞.

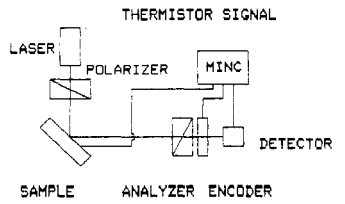

Figure 3. Schematic of the automated ellipsometer.

Table I

$10^{-6}\bar{M}_w$	$\bar{M}_w/\bar{M}_n$	supplier
1.8	1.30	Pressure Chemical Co.
3.84	1.04	Toyo Soda Co.
8.42	1.17	Toyo Soda Co.
20	<1.20	Pressure Chemical Co.

$K(r)$ by its preaveraged value $K(\langle r^2\rangle^{1/2})$. This results in the following set of algebraic equations that must be solved in order to obtain the moment $\langle y\rangle^2$:

$$\langle y^2\rangle = 1/2N\xi \tag{7}$$

$$\langle r^2\rangle = (3/2N\xi)[1 + (\alpha^2/24\xi^2)] \tag{8}$$

$$\xi = 1/(1 - \langle r^2\rangle) \tag{9}$$

Figure 2 is a plot of $l = \{\langle y^2\rangle/\langle y^2\rangle_0\}^{1/2}$ as a function of α, where $\langle y^2\rangle_0$ is the value of that moment for $\alpha = 0$. The calculations have been carried out for various values of N where the limit as $N \to \infty$ represents the case of a constant spring coefficient. The consequence of introducing a nonlinear spring coefficient is to make the spring finitely extensible up to a limit of the contour length. As the spring deforms toward this upper limit the distortion is suppressed and the bead is forced downward toward the surface resulting in a lower thickness as the velocity gradient is increased.

Experimental Section

Materials. Four linear polystyrene samples of high molecular weight were used. The characteristics of the samples are given in Table I. The solvent used was reagent grade cyclohexane. The substrate consisted of optically flat hard chrome electroplated onto steel disks. Prior to each adsorption, the chrome mirrors were cleaned by polishing them with Linde A or Linde B polishing compound in order to remove any adsorbed polymer film from previous experiments and then flushing them with a stream of distilled water. The mirrors were then immersed in 9% NaOH aqueous solution for 20 min, washed in distilled water, dried, and finally passed 10 times through the flame of a gas burner immediately before assembling the flow cell.

Ellipsometry. Figure 3 is a schematic of the experimental arrangement. The automated ellipsometer is essentially the equivalent of that described by Hauge and Dill.[6] The light intensity is detected by a power meter and that signal is sent to the A/D converter of a Digital Equipment Corp. MINC 11/23 system. An encoder attached to the rotating analyzer sends a trigger signal to a Schmitt trigger on the clock controlling the A/D converter. The signal initiates acquisition of 256 data points over a single revolution of the analyzer. Also sent is a signal from a thermistor probe within the flow cell in order to monitor the liquid temperature.

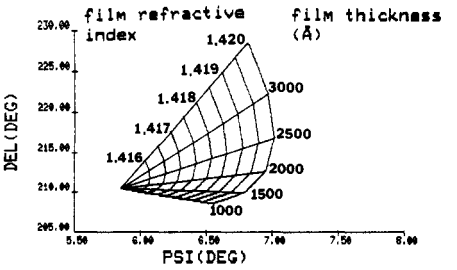

Figure 4. Calculated ellipsometric angles (Ψ, Δ) as functions of film thickness and film refractive index. The calculation was for a polystyrene/cyclohexane/chrome system, $\Psi = 80°$, $\lambda = 6328$ Å, $n_0 = 1.415$, and triple reflection between chrome mirrors.

The intensity at the detector can be shown to be

$$I = |E_1^2| = |E_0^2|a_0(1 + a_2 \cos 2\omega t + b_2 \sin 2\omega t) \tag{10}$$

where

$$a_0 = (|R_{pp}^2| + |R_{ss}^2|)/2 \tag{11a}$$

$$a_2 = (|R_{pp}^2| - |R_{ss}^2|)/(2a_0) \tag{11b}$$

$$b_2 = (R_{pp}^* R_{ss} + R_{pp} R_{ss}^*)/(2a_0) \tag{11c}$$

The frequency ω appearing in eq 10 is the angular velocity of the rotating analyzer. Here R_{pp} and R_{ss} are the complex reflection coefficients of the sample surface for light parallel and normal to the plane of incidence, respectively. The ratio of reflection coefficients R_{pp}/R_{ss} is usually expressed in terms of the ellipsometric angles Ψ and Δ through the following expression:

$$R_{pp}/R_{ss} = \tan \Psi \exp(i\Delta) \tag{12}$$

By use of eq 11 it is straightforward to show that

$$a_2 = -\cos 2\Psi \tag{13}$$

$$b_2 = \sin 2\Psi \cos \Delta \tag{14}$$

The coefficients a_2 and b_2 are determined directly from a fast Fourier transformation of the light intensity measured over a single revolution of the rotating analyzer. Once a_2 and b_2 are known, Ψ and Δ can be determined immediately by using eq 13 and 14. These determinations can be made once every 10 s with the present system and the angular velocity of the analyzer (1 Hz).

Knowledge of Ψ and Δ specifies the ratio R_{pp}/R_{ss} of the surface reflecting the light. For the reflection off of a clean substrate, the real and imaginary parts of the refractive index (n_s, k_s) can be calculated from Ψ and Δ. If the substrate also contains a film, the film thickness and refractive index can be determined by using the calculated optical properties of the clean substrate mentioned above in addition to the refractive index of the solution above the film n_0 and assuming that the film is nonabsorbing (in other words, that the film refractive index is real). The determination of the film thickness d and refractive index n_f involves a nontrivial inversion of a transcendental equation derived from classical electrodynamics. The details of the analysis can be found elsewhere[7] and will not be repeated here. Figure 4 shows a typical relationship between Ψ and Δ for a series of film thicknesses (d = 0–3500 Å) and film refractive indices ($\Delta n = n_f - n_0$ = 0.001–0.005). The calculation was performed for the case of an adsorption cell at the angle of incidence $\phi = 80°$, and monochromatic light (λ = 6328 Å) triply reflected off of two parallel chromium mirror surfaces with the refractive index of the solution above the film was taken to be that of cyclohexane ($n_0 = 1.415$).

The measured thickness and refractive index of the film can be combined to estimate the adsorbance A (g/cm^2). This calculation assumed n_f is a linear superposition of the refractive index of the polymer and of the solvent making up the film. The following equation is used:

$$A = (n_f - n_0)d/(dn/dc) \tag{15}$$

where dn/dc is the refractive index increment of the polymer in the solvent and is 0.168 cm^3/g for polystyrene in cyclohexane at the Θ condition. The solvent refractive index was used irrespective

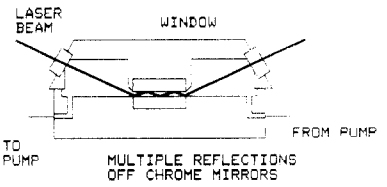

Figure 5. Flow cell.

of the concentration of solution and resulted in less than 0.5% error in the determinations of d and A even at the highest concentration of 1500 ppm. This is far less than the experimental errors of about 3%. The results shown in Figure 4 are, therefore, independent of polymer molecular weight and bulk concentration. It should also be mentioned that the film thickness which is measured with ellipsometry is an average over the distribution of segments above the surface. It has been common in the past[8] to report a root-mean-square thickness d_{rms} which is related to the measured thickness by $d_{rms} = d/F$, where F is a constant factor which is specific to the distribution used. For an exponential distribution $F = 1.5$ and for a Gaussian distribution $F = 1.74$.

Flow Cell. Figure 5 shows a drawing of the flow cell, which is similar in some respects to the one used by Stromberg et al.[8] The cell consists of two chromium mirrors which are parallel and facing each other. The mirrors serve both as boundaries for the flow and as adsorption surfaces. Each mirror rests within an aluminum base or lid, respectively, and the base and the top lid are themselves squeezed between two aluminum blocks which support circulating water from a constant temperature bath. The top lid has two fused-quartz windows of low birefringence and contains an opening for insertion of a thermistor directly in contact with the liquid. The two blocks are pressed together tightly by using a Viton o-ring to seal the unit. The gap between the two mirrors can be inferred by measuring the gap between the base and the lid with a filler gauge set and was measured to be 0.06 ± 0.004 cm. The flow path is 1.40-cm long and 1.91-cm wide. The first reflection point is located at 0.35 cm from the leading edge. Apparent velocity gradients $\dot{\gamma}$ were calculated by assuming a fully developed velocity profile ($\dot{\gamma} = 6Q/WB^2$, Q being volume flow rate, B the gap thickness, and W the width). At high flow rates entrance length effects will cause the apparent velocity gradients calculated in this manner to be slightly lower than the actual gradients existing in the cell. In the case of highest Reynolds number, the actual velocity gradient at the first reflection point is estimated to be 15% higher than the apparent velocity gradient.[9] Since the measured Ψ and Δ are the average of three reflections, the overall discrepancy would be less than 15% for the worst case. With our current pump capacity and the gap of about 0.06 cm, we can study flowing systems with apparent velocity gradients up to 7800 s^{-1} at Reynolds numbers not exceeding 250.

Sensitivity studies show for thick films ($d = 3000$ Å) an angle of incidence $\phi = 80°$ is superior to the conventional choice of $\phi = 70°$. The configuration of the cell with $\phi = 80°$ and the gap of 0.06 cm results in a triple reflection of light between the mirrors. The analysis of the experiment will still follow that outlined in the previous section but with the values for Ψ and Δ for a single reflection being replaced to $\psi^{[m]}$ and $\Delta^{[m]}$ for the case of m multiple reflections by

$$(\tan \Psi)^m \exp(im\Delta) = \tan \Psi^{[m]} \exp(i\Delta^{[m]}) \qquad (16)$$

The current design of the flow cell allows us to study a wide range of polymer/solvent pairs. Since the light only passes through quartz windows at normal incidence, there is no problem of mismatching of refractive indices.

Procedure. (1) Adsorption from Quiescent Solution. The refractive index ($n_s - ik_s$) of the freshly cleaned chrome mirrors was first measured under cyclohexane. The polymer solution was then introduced into the cell by means of a hypodermic syringe. The measured values of Ψ and Δ were displayed on a terminal screen as functions of time and stored in the computer along with temperature readings for later analysis. Figure 6 represents the adsorption kinetics of the 20 million molecular weight sample. The bulk solution concentration of polystyrene was 700 ppm, which is known to be higher than that required to reach the plateau region of the isotherm for this particular system from the

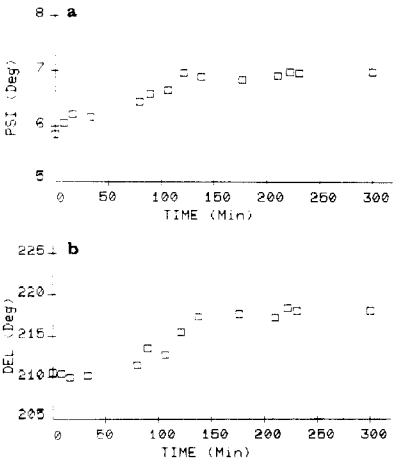

Figure 6. Measured ellipsometric angles (Ψ, Δ) as functions of time. Same system as in Figure 4 with polymer molecular weight = 20 × 10^6, concentration = 700 ppm, and temperature = 34.8 °C: (a) Ψ (PSI) vs. time; (b) Δ (DEL) vs. time.

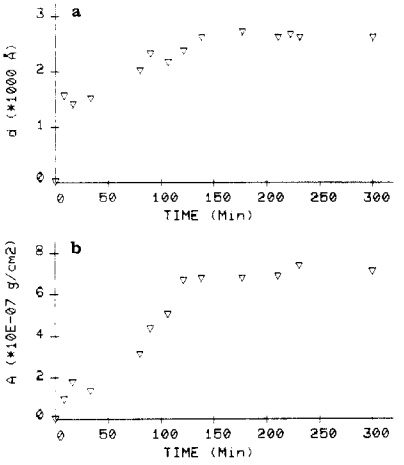

Figure 7. (a) Film thickness as a function of time. (b) Adsorbance as a function of time.

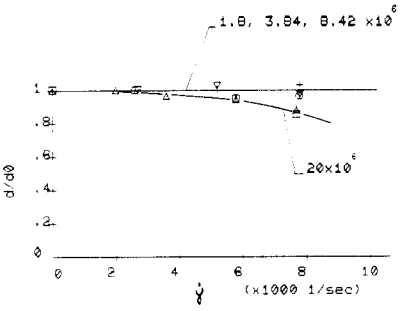

Figure 8. Measured film thickness ratio as a function of apparent velocity gradient $\dot{\gamma}$. □ refers to decreasing $\dot{\gamma}$ from the highest value. Δ is for increasing the velocity gradient to its highest value. +, ▽, and ○ are for the films of molecular weights of 1.8 × 10^6, 3.84 × 10^6, and 8.42 × 10^6, respectively.

previous work of Takahashi et al.[10] Similar concentration levels were also chosen to ensure saturated films of high surface coverages for the three other samples. The temperature was kept at 34.8 ± 0.1 °C, which is the Θ temperature of polystyrene in cyclohexane.

(2) Flow Effect Studies. The solution was kept in place in the cell over a period of 1 day at which time the solution was displaced by pure solvent and the flow of solvent was initiated. For the 20 million molecular weight sample we have performed the flow studies at various velocity gradients by either starting from the highest possible flow rate and proceeding to lower ones (indicated by the square symbol in Figure 8) or starting from lower flow rates and proceeding to the highest one (triangular symbol

in Figure 8). For the three lower molecular weight samples three specific velocity gradients ($\dot{\gamma}$ = 2600, 5200, and 7800 s^{-1}) were studied. At each velocity gradient, the pump was turned on and off 3 to 5 times and the ellipsometric angles Ψ and Δ were measured both during the flow and following the cessation of flow. The film thickness and adsorbance were then evaluated by using the average Ψ and Δ values.

Results and Discussion

Adsorption Kinetics. Although Takahashi et al.[10] have reported kinetics data on the polystyrene/cyclohexane/chrome system over an extensive range of molecular weight, we will present our results of the 20 million molecular weight sample, as our system represents a higher molecular weight sample than previously studied. By use of the measured values of Ψ and Δ at each point in time, Figure 4 was used to determine the film thickness and adsorbance as functions of time. The results are plotted in Figure 7, parts a and b. Immediately after introduction of the polymer solution the thickness jumped to 1500 Å and reached a steady state value of 2600 Å in approximately 2.5 h. The adsorbance, on the other hand, followed a much slower initial approach to its steady state value of 7×10^{-7} g/cm^2.

It is of interest to compare our results for thickness and adsorbance against those reported by Takahashi et al.[10] Those authors reported a linear relationship of the thickness with the square root of molecular weight. If their data are extrapolated to a molecular weight of 20 million and if their reported root-mean-square thickness is multiplied by their factor of 1.5 (i.e., an exponential distribution was assumed), a value of 2850 Å is obtained, which is within 9% of the value we observed. They reported that the adsorbance for molecular weight greater than about $^1/_2$ million should be independent of molecular weight at a value of approximately 5×10^{-7} g/cm^2. The level of agreement between the two sets of data is acceptable and within the expected precision of the technique. In addition, differences in surface roughness and surface cleaning procedures may lead to intrinsically different adsorption characteristics.

The thickness of 2600 Å suggests a weakly adsorbed monolayer surface coverage. When the adsorbance is divided by the thickness, the mean polymer concentration in the adsorbed layer is estimated to be 2.7×10^{-2} g/cm^3. As pointed out by Takahashi et al.,[10] this concentration is roughly 4 times larger than the average segment density of an isolated, random coil.

Flow Effects. Figure 8 is a plot of the ratio of the measured film thickness d at any given velocity gradient to the thickness d_0 at zero flow. The plot consists of the results for two separate adsorbed films of the 20 million molecular weight sample and one film each of the three lower molecular weight samples. As discussed earlier, for the 20 million molecular weight sample the data described by the triangular symbol refer to the case where the velocity gradient was sequentially increased to its highest value whereas the square symbol is for the case where the velocity gradient was decreased from its highest value. All three adsorbed layers of lower molecular weight samples showed no significant changes in film thickness over the whole range of velocity gradients applied in this study. On the other hand, for the 20 million molecular weight sample very good agreement was found between the two sets of data, with the overall trend showing a monotonic decrease in thickness as the velocity gradient surpassed about 2000 s^{-1}. In no cases were irreversible flow-induced changes in either the thickness or adsorbance observed. Over the duration of the entire flow study, however, we noticed a slow, irreversible desorption of the polymer into the bulk solvent. Similar desorption has been observed by using radiotracer technique in the past by Grant et al.[11] In the studies reported here, the flow field was only applied for short durations of time (10 s) and then arrested. Studies are currently being carried out in order to determine the rate of desorption under conditions of flow sustained over long periods of time.

The measured reponses for the thicknesses are in general agreement with the predictions of the simple bead-and-spring model. Given choices for the adjustable parameters N and β/K_0, the data could be fit reasonably well with the model. However, due to its simplicity and the arbitrary choice for the spring function, only qualitative comparison will be given here. The model indicates that the film thickness should begin to decrease when the product of the velocity gradient and the principal relaxation time of the adsorbed segments reaches a certain value which depends on the length of the segments. The failure of the lower molecular weight samples to show any flow-induced thickness changes can therefore be simply related to their faster relaxation times compared with that for the 20 million molecular weight sample. For the films of the 20 million molecular weight sample the thickness is essentially constant over a wide range of velocity gradients before it begins to decrease. On the basis of the model, this decrease can be interpreted as a manifestation of an extension of the chains which approaches the upper limit of the extension (which for a dangling end is simply the contour length of the chain). The hydrodynamic forces do not, however, become large enough to rupture the chains or tear them from the surface over the short time period the flow was applied.

It is of interest to compare the results obtained using ellipsometry with those from the hydrodynamic studies of Gramain and Myard[1] and Cohen and Metzner.[2] In making such comparison, however, several matters regarding the differences in the two techniques must be examined. As pointed out earlier, the two techniques provide different measures of the average film thickness. The film thickness measured by ellipsometry is an average over the entire segmental distribution above the surface. The hydrodynamic method, on the other hand, is considered to be more sensitive to those dangling ends and loops which extend furthest from the surface. For very high-velocity gradients where the adsorbed layer becomes substantially deformed, it is possible that the friction factor of larger segments (which most significantly contribute to the resistance) may no longer be constant and become conformation dependent. It has been argued to be the case for isolated, free polymer chains by de Gennes[12] and Hinch.[13] This could partly explain the unusual dilatant behavior of the hydrodynamic thicknesses reported by Gramain and Myard.[1]

Other factors that complicate the comparison with past hydrodynamic studies are the complex flow geometries involved with the porous media used by Gramain and Myard[1] and the large polymer concentrations used by Cohen and Metzner.[2] The flows through porous media may involve a mixture of both shear and extensional flows, which may be the basis for the dilatant behavior observed by Gramain and Myard.[1] A reduction of hydrodynamic thickness instead of dilation was observed by Cohen and Metzner[2] for the case of capillary flow.

Our results are in general agreement with a decrease in adsorbed layer thickness but in a qualitatively different manner than that reported by Cohen and Metzner.[2] They reported the effective hydrodynamic thickness decreased by as much as 50% and with a much steeper initial slope

at lower velocity gradients than for the mean thickness measured with ellipsometry. That work represented the first attempt at measuring the properties of an adsorbed layer beneath a flowing solution whereas this work and previous studies have involved the flow of pure solvent.

Acknowledgment. This work was supported by the National Science Foundation under the NSF Initiation Grant CPE8105497. We are also grateful for financial support by the Institute for Energy Studies at Stanford University.

Registry No. Polystyrene (homopolymer), 9003-53-6.

References and Notes

(1) Gramain, Ph.; Myard, Ph. *Macromolecules* **1981**, *14*, 180.
(2) Cohen, Y.; Metzner, A. B. *Macromolecules* **1982**, *15*, 1425.
(3) DiMarzio, E. A.; Rubin, R. J. *J. Polym. Sci., Polym. Phys. Ed.* **1978**, *16*, 457.
(4) Fuller, G. G. *J. Polym. Sci., Polym. Phys. Ed.* **1983**, *21*, 151.
(5) Warner, H. R., Jr. *Ind. Eng. Chem. Fundam.* **1972**, *11*, 379.
(6) Hauge, P. S.; Dill, F. D. *IBM J. Res. Dev.* **1973**, *17*, 472.
(7) Azzam, R. M. A.; Bashara, N. M. "Ellipsometry and Polarized Light"; North Holland: Amsterdam, 1979.
(8) Stromberg, R. R.; Tutas, D. J.; Passaglia, E. *J. Phys. Chem.* **1965**, *69*, 3955.
(9) Sparrow, E. M.; Lin, S. H.; Lundgren, T. S. *Phys. Fluids* **1964**, *7*, 338.
(10) Takahashi, A.; Kawaguchi, M.; Hirota, H.; Kato, T. *Macromolecules* **1980**, *13*, 884.
(11) Grant, W. H.; Smith, L. E.; Stromberg, R. R. *Faraday Discuss. Chem. Soc.* **1975**, *No. 59*, 209.
(12) de Gennes, P.-G. *J. Chem. Phys.* **1974**, *60*, 5030.
(13) Hinch, E. J. Proceedings of the Symposium on Polymer Lubrification, Brest, 1974.

Statistical Thermodynamics of Short-Chain Molecule Interphases. 1. Theory

Ken A. Dill and Robert S. Cantor*

Department of Pharmaceutical Chemistry, School of Pharmacy, University of California, San Francisco, California 94143. *Received May 9, 1983*

ABSTRACT: Amphiphilic molecules comprised of a polar head and hydrocarbon tail associate in aqueous environment to form micelles, vesicles, bilayers, or other aggregates, consisting of hydrocarbon domains separated from the water regions by the head groups. Statistical theory for the hydrocarbon "interphase" region of such systems is developed, extending previous work to account for chain bending energies and to allow prediction of thermodynamic as well as structural properties. Expressions for the statistical weights of chain configurations and a configurational partition function are obtained subject to the constraint of approximately constant density within the hydrocarbon core, which is a consequence of strongly attractive isotropic van der Waals forces, balanced by hard-core steric repulsive forces. Expressions for positional and orientational probability distributions are derived.

Amphiphilic molecules comprised of a polar head and hydrocarbon tail associate in aqueous environment to form micelles, vesicles, bilayers, or other aggregates, consisting of hydrocarbon domains separated from the water regions by the head groups. The density within the hydrocarbon core is approximately equal to that within bulk liquid alkane phases, a consequence of strongly attractive isotropic van der Waals forces which are balanced by hard-core, short-range steric repulsive forces.[1] The constraints imposed by the different solubilities of head groups and tails in water and by the balance of intermolecular forces severely restrict the configurations available to the molecules. As a consequence, the degree of structural order within the hydrocarbon domain is not constant; rather, it varies over molecular dimensions along a coordinate axis determined by system geometry.[2,3] For example, in lipid bilayers, the hydrocarbon chains have greater orientational order near the heads than near the terminal methyl groups.[4] Such systems, herein termed "interphases", differ significantly from other condensed polymer phases such as liquids, crystals, and nematic liquid crystals, in which the degree of order is independent of spatial position.

Statistical mechanical theory has previously been developed which accounts for these constraints and which predicts structural properties of interphases, assuming freely jointed hydrocarbon chains.[2,3] In the present work, we extend the theory to take into account chain bending energies and also to allow the prediction of thermodynamic properties of interphases.

The Model

Subject to the continuity of the hydrocarbon chains and the nearly constant density within the interphase, the configurations of the chains may be systematically enumerated through use of a spatial lattice. The volume of space occupied by the interphase hydrocarbons is partitioned into nonoverlapping sites of equal volume, each of which may contain one chain segment. Chains are comprised of $n + 1$ "segments", occupying $n + 1$ contiguous sites, and thus of n "bonds" connecting the segments. In order that all bonds be of equal length, the sites must be isodiametric. Thus, the chain width dictates the segment length; for polymethylenic chains, each segment is comprised of approximately 3.6 CH_2 groups. For a planar monolayer or bilayer, sites may be considered to occur in planar layers, numbered $i = 1, 2, ..., n$ from the interface. For nonplanar interphases, layers are concentric with the interface and labeled in the same manner, and the number of sites per layer, N_i, varies with layer index, i.

Let J_1 be the total number of chains; then $\sigma_1 = J_1/N_1$ is the surface density of chains, where $0 \leq \sigma_1 \leq 1$. Assuming that the polar head groups are localized at the water/hydrocarbon interface, the first segments of each of the J_1 chains must all be in the first layer. We assume

0024-9297/84/2217-0380$01.50/0